NMR Investigation of Chain Deformation in Sheared Polymer Fluids

A. I. Nakatani,† M. D. Poliks,‡ and E. T. Samulski*

Department of Chemistry and Institute of Materials Science, University of Connecticut, Storrs, Connecticut 06268

Received August 1, 1989; Revised Manuscript Received November 20, 1989

ABSTRACT: *Rheo-NMR*, the use of nuclear magnetic resonance to monitor the behavior of entangled polymers subjected to shear, is here proposed as a new experimental technique for studying the microscopic response to shear-induced anisotropy in *bulk* polymers. A cone and plate rheometer designed to operate in a standard NMR probe is described. This apparatus permitted observations of changes in the residual anisotropic proton dipolar interactions. Proton NMR line widths increase in a reproducible manner when melts of poly(isobutylene) and poly(dimethylsiloxane) are sheared. The NMR spectral broadening is associated with a redistribution of the primitive chain path (the tube axis orientational distribution) by the shear deformation; the initial response and the decay to the equilibrium distribution after cessation of shear are, however, inexplicably longer than that anticipated from rheological measurements, i.e., longer than observed stress relaxation times for these melts. A shear-induced phase transformation in poly(vinyl methyl ether)–water mixtures is demonstrated with the apparatus. These findings illustrate the potential and feasibility of rheo-NMR studies of bulk polymers.

Introduction

Methods for deriving quantitative, microscopic information about polymer chains as they respond to a macroscopic perturbation enables one to advance molecular descriptions of bulk behavior. In the rheology of polymer fluids, there are very few experimental options for investigating microscopic aspects of bulk samples. For example, high extinction coefficients limit the traditional methodologies (infrared dichroism, optical birefringence) to thin samples; hence, surface phenomena may complicate such measurements. Scattering techniques (small-angle neutron and X-ray), while sampling the bulk material, give limited information about local intrachain behavior. By contrast, nuclear magnetic resonance (NMR) is an inherently insensitive technique and bulk samples are usually examined to improve signal-to-noise. Moreover, NMR interactions are local in nature and provide information at the level of the chain's primary structural elements, the chemical bonds. This combination of features in conjugation with earlier work in our laboratory that used NMR to probe orientation phenomena in deformed networks prompted us to consider its utility for studying sheared polymer melts. When the macromolecules are above their entanglement MW, the melt might be viewed as a deformed, transient network.

Preliminary observations indicate that rheo-NMR—monitoring shear-induced anisotropic NMR interactions in entangled polymer fluids—is a viable experimental technique. In this report we describe an apparatus that generates uniform shear fields of variable stress intensity in the active sample volume of a nuclear magnetic resonance spectrometer having a transverse magnetic field. Herein we focus on the design and construction of the rheometer which functions within the severe practical limitations of commercially available rf probes used in a conventional NMR spectrometer. The major design limitations are a small active volume in the rheometer (<0.01 cm^3) and the materials restrictions (the rheometer must be constructed from non-NMR-active and non-metallic components). The first limitation merely translates into poor signal-to-noise (which can be partially compensated by signal averaging), and the second limitation may be virtually neutralized by constructing the rheometer from engineering polymers (nylon, Delrin, polyimide, etc.). It should be emphasized that there are negligible complications when observing highly mobile nuclei of the polymer fluid (high-resolution NMR) in the presence of the very broad background signals from the solid engineering polymers (wide-line NMR). The description of the rheometer we designed is preceded by a summary of the relevant NMR theory and experiments that initially motivated us to explore rheo-NMR as a tool for interrogating bulk polymer samples under stress. We conclude with some preliminary findings obtained with proton NMR on poly(isobutylene) and poly(dimethylsiloxane) melts and a poly(vinyl methyl ether)–water mixture subjected to simple shear.

Background

The methodology we employ derives from NMR studies of liquid crystals. In these intrinsically anisotropic fluids rapid but orientationally biased molecular reorientation and self-diffusion average second-rank tensorial nuclear interactions in very specific ways.[1] The two most frequently investigated interaction tensors are as follows: 1) $\mathbf{D}^{ij}$, the dipolar interaction tensor expressing *direct* dipole–dipole coupling between nuclei i and j (usually protons) on a given molecule; (2) $\mathbf{q}^i$ the quadrupolar interaction tensor expressing the coupling between the nuclear quadrupole moment and the electric field gradient at nucleus i (usually a deuteron). Both are traceless tensors ($\sum A_{nn} = 0$, where $\mathbf{A} = \mathbf{D}, \mathbf{q}$); hence these interactions are averaged to zero by molecular motion in isotropic liquids. By contrast, in a liquid crystal the averages of $\mathbf{D}$ and $\mathbf{q}$ are non zero and, coarsely speaking, $\langle \mathbf{A} \rangle$ acquires the symmetry of the liquid crystal phase which, in turn, is determined by the motionally averaged molecular arrangement in these ordered fluids. In the uniax-

* To whom correspondence should be addressed at the Department of Chemistry, CB# 3290, University of North Carolina, Chapel Hill, NC 27599-3290.

† National Institute of Standards and Technology (formerly National Bureau of Standards), Polymer Division, Gaithersburg, MD 20899.

‡ Department of Chemistry, Washington University, St. Louis, MO 63130.

0024-9297/90/2223-2686$02.50/0

ial nematic phase, for example, $\langle \mathbf{A} \rangle$ expressed in a frame within a uniform volume element of the nematic is conveniently given in terms of the single value S, the principal element of an orientational order tensor, $\mathbf{S}$:

$$\langle \mathbf{A} \rangle = AS \begin{bmatrix} (-1/2) & 0 & 0 \\ 0 & (-1/2) & 0 \\ 0 & 0 & 1 \end{bmatrix} \quad (1)$$

where A is the principal element of the interaction tensor in its local principal axis system (PAS) and $S = \langle P_2(\cos\theta) \rangle$ gives the average orientation of the PAS relative to $\mathbf{n}$. That is, θ is the time-dependent angle between the nematic director $\boldsymbol{n}$ and the relevant interaction vector of A. D or q (i.e., A) is often referred to as the coupling constant. For $\mathbf{D}$ and $\mathbf{q}$, the vectors are respectively the internuclear vector $\mathbf{r}_{ij}$ and the covalent bond vector to the quadrupolar nucleus; when the latter is the deuteron covalently attached to carbon, an axially symmetric electric field gradient (EFG) tensor is assumed in the PAS with the principal value of the EFG tensor along the C–D bond. The brackets $\langle\ \rangle$ indicate a time average over the rapid (anisotropic) molecular motion in the liquid crystal. Usually values for S in the range of 0.3–0.8 are found in low molar mass, thermotropic liquid crystals.

Intermolecular nuclear interactions are completely averaged in nematic melts by molecular diffusion; therefore only partially averaged *intramolecular* interactions are present. These interactions depend on the orientation of $\mathbf{n}$ in the laboratory frame defined by the spectrometer magnetic field; they appear as additional splittings in the high-resolution NMR spectra

$$\Delta\nu \approx ASP_2(\cos\Omega) \quad (2)$$

where Ω is the angle between $\boldsymbol{n}$ and the spectrometer magnetic field $\mathbf{B}$. It is clear from eq 2 that in uniaxial fluid phases a measurement of the magnitude of the splitting $\Delta\nu$ together with the independently determined coupling constant (D or q) yields in a very straightforward manner, the *magnitude* of the order parameter characterizing the average orientation of the interaction vector with respect to $\boldsymbol{n}$. (If S is greater than 0.5, then by definition its sign is positive which implies that on average the interaction vector is parallel to $\boldsymbol{n}$.)

Perhaps the most striking feature of the NMR spectra of liquid crystals is the very large magnitudes of these dipolar and quadrupolar splittings: $\Delta\nu$ often is observed to be in the range 10^3–10^5 Hz. This is due in part to the high orientational order exhibited by liquid crystals ($S > 0.3$). For the most part, however, large splittings arise because the coupling constants are very large: For a pair of protons separated by a distance r, $D = \gamma^2 h/4\pi^2 r^3 = 120\,000/r^3$ Hz Å^3; the constants γ and h are the magnetogyric ratio and Planck's constant, respectively.[2] In the case of a deuterium-labeled carbon, $q = e^2qQ/h = 165\,000$–$195\,000$ Hz, where eq is the principal value of the EFG tensor and Q is the quadrupole moment of the deuteron.[2] Moreover, since nominal high-resolution NMR conditions are fulfilled in these anisotropic liquids, $\Delta\nu$ values of the order of 1 Hz may be readily resolved. Hence eq 2 in conjunction with the large coupling constants implies that deviations from isotropy as small as $\langle P_2(\cos\theta) \rangle = 10^{-4}$–$10^{-5}$ can be readily determined by measuring these partially averaged tensorial NMR interactions. In order to use NMR to study deformed polymers, it is necessary to have a methodology that is sensitive to very low degrees of orientational order. This is due in part to the small-chain extensions encountered in mechanically deformed samples and the very effective, nearly isotropic motional averaging processes within polymer chains.

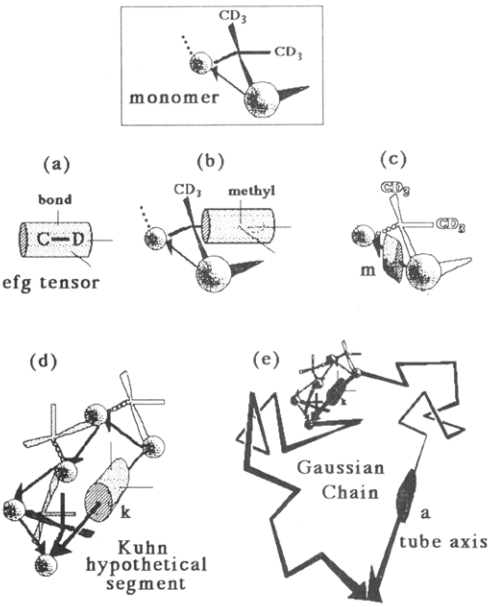

Figure 1. A schematic diagram of the various intramacromolecular motional averaging processes that occur in a Gaussian chain composed of labeled, idealized monomer. The orientation of the (assumed) uniaxial (averaged) EFG tensor is indicated by the shaded cylinder for each stage (a–e) of the hierarchical model.

The manner in which nuclear dipolar and quadrupolar interactions are averaged in polymer fluids can be approximated by a hierarchy of averaging processes that take place in polymer chains. This hierarchy is depicted in Figure 1 wherein for simplicity, the quadrupolar interaction is considered in an idealized polymer. The chain is composed of a sequence of hypothetical monomer units each with a pair of deuterium-labeled methyl groups. The assumed axially symmetric EFG tensors (shown as shaded cylinders in their respective PAS) are successively averaged, each in turn as one moves from monomer to segment to chain. This averaging becomes more efficient as one ascends the hierarchical scale because of the corresponding increase in the number of internal degrees of freedom at each scale. Figure 1a: The largest interaction is for the static uniaxial EFG tensor defined on the C–D bond. In this local PAS the static quadrupolar interaction for an aliphatic deuteron applies in the absence of intra- and extramolecular motion yielding a value for $\Delta\nu = {}^3/_2 A\langle P_2(\cos\theta) \rangle = 250\,000$ Hz where $A = q$ and the C–D bond is parallel to the magnetic field ($\theta = 0°$). Figure 1b: Intramonomer motion (rotation about the local C_3 axis of the methyl; tetrahedral geometry assumed) reduces the interaction tensor by a simple factor, $\langle \mathbf{A} \rangle_{C_3} = |P_2(\cos 109.5°)|A = 1/3A$ and redefines the PAS on the monomer to be coincident with the methyl C_3 axis. Figure 1c: Transformation of the tensor to the monomer axis $\mathbf{m}$—the "chord" connecting next nearest atoms in the backbone of the chain for the indicated monomer—again reduces the interaction magnitude by a factor $\langle \mathbf{A} \rangle_{\mathbf{m}} = |P_2(\cos 90°)|\langle \mathbf{A} \rangle_{C_3} = {}^1/_2\langle A \rangle_{C_3}$ for the geometry illustrated (the C_3 axis is perpendicular to $\boldsymbol{m}$ and axial symmetry is assumed about $\boldsymbol{m}$). Figure 1d: Isomerization of the monomer within a hypothetical Kuhn segment $\boldsymbol{k}$ consisting of several monomers yields a further averaged interaction tensor with its corresponding principal value along $\boldsymbol{k}$ (uniaxial isomerization of $\boldsymbol{m}$ about $\boldsymbol{k}$ is assumed). The extent of the latter averaging would depend on the details of the dihedral angle energetics, the constraints within the monomer primary structure (bond lengths and

valence angles), and the number of monomer units per hypothetical segment. Explicit calculations of this average may be carried out by using the rotational isomeric state approximation and suggest that a reduction of the interaction on the order of $\langle \mathbf{A} \rangle_k \approx {}^1/_{10} \langle \mathbf{A} \rangle_m$.[3] Figure 1e: Librational and diffusional motion of segments further averages the interaction tensor to a residual interaction directed along the polymer chain's primitive path (or tube axis $\boldsymbol{a}$ in an entangled melt). The resulting small residual interaction ($\langle \mathbf{A} \rangle_a$ is on the order of 1% of the initial static interaction A) is only averaged to zero if $\boldsymbol{a}$ reorients isotropically on the time scale determined by the inverse of the partially averaged interaction $\langle \mathbf{A} \rangle_k$. Therefore, in order for second rank tensorial NMR interactions to vanish in an entangled melt the tube axis $\boldsymbol{a}$ would have to reorient, or equivalently, the labeled monomer would have to successively sample a sufficient number of arbitrarily oriented tubes by self-diffusing along the chain's primitive path (reptating). Above T_g in very fluid polymer phases, dipolar and quadrupolar interactions are effectively averaged to zero by the convolution of the processes depicted in the idealized hierarchical averaging scheme shown in Figure 1. Consequently, very fluid polymer melts are isotropic on the longest NMR-defined time scale (for times $t > (\langle \mathbf{A} \rangle_a)^{-1}$).

Consider the situation when $\boldsymbol{a}$ is not isotropically distributed and its motion is constrained as in the case of a chain between cross-links (or topological entanglements) in a deformed elastomer network. Above T_g the segmental motions within the tethered, distended chain are anisotropic and the averaging of dipolar and quadrupolar interactions is incomplete. In fact, for uniaxially deformed networks the intrachain (intratube) interactions are averaged in a manner reminiscent of that in uniaxial liquid crystals. Equation 2 is applicable as $\langle \boldsymbol{A} \rangle$ assumes the symmetry of the deformation imposed on the network. Qualitatively speaking, $\langle \boldsymbol{A} \rangle$ is determined by the residual segmental orientational order in the network. This may be expressed with an order parameter S related to the average orientation of a hypothetical chain segment $\boldsymbol{k}$ relative to the chain vector $\boldsymbol{a}$. According to classical (Gaussian) descriptions of polymer chains, very small orientational order parameters are expected for chain segments in deformed elastomer networks. S is predicted to be inversely proportional to N, the number of segments spanning $\boldsymbol{a}$, and proportional to the strain on the network. In networks subjected to uniaxial extension or compression, S is proportional to $(\lambda^2 - \lambda^{-1})$, where the deformation ratio $\lambda = L/L_0$ is the ratio of the macroscopic dimensions of the network in the strained and unstrained states. For plausible values of N and λ, S is predicted to lie in the range of 10^{-2}–10^{-5}.

From an experimental feasibility viewpoint, the small degree of orientational order is offset by the large magnitudes of proton dipolar and deuterium quadrupolar coupling constants. Thus NMR is a suitable technique for monitoring segmental orientation in polymer networks and Deloche and Samulski[4] demonstrated the utility of NMR in this capacity in 1981. Using deuterated swelling agents in cross-linked rubber they showed that the deuterium NMR quadrupolar splitting of the swelling agent is a function of the strain imposed on the swollen network. Direct observation of the chain segment orientational order was reported in subsequent NMR investigations carried out on deuterium-labeled networks.[5] Labeled oligomers swollen into networks have been investigated,[6] and studies of network characteristics (degree of cross-linking and swelling)[7] have also exploited the ^{2}H NMR technique.

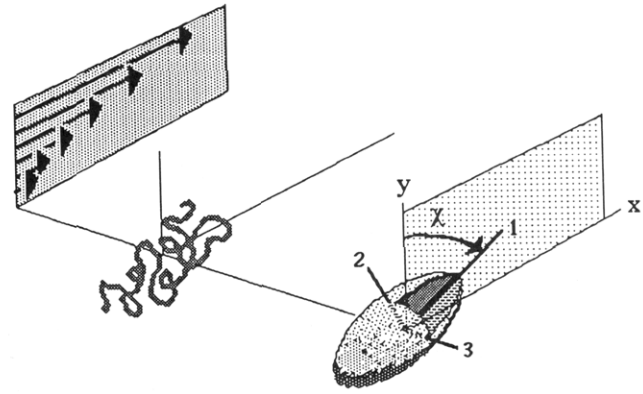

Figure 2. An idealized representation of the deformation of a polymer chain under simple shear. The velocity gradient is in the x–y plane and the shaded ellipsoid represents the chain's radius of gyrations tensor.

Cognizant of the potential of the NMR technique for observing very small degrees of orientational anisotropy, we were motivated to consider extending this type of NMR experiment to entangled polymer fluids (high molecular weight polymer melts or concentrated solutions) undergoing a shear deformation. It was anticipated that there would be sufficient sensitivity to detect the small steady-state segmental anisotropy induced in such flowing fluids (transient networks in the case of chains above the entanglement molecular weight). What is anticipated is schematically shown in Figure 2. The chain's radius of gyration is depicted as an ellipsoid due to the extensional component of the stress acting on a chain subjected to the velocity gradient in simple shear. An anisotropic distribution of the chain's primitive path segments (successive tubes defined by the test chain's librational diffusion) spanning dynamic entanglements should yield an incompletely averaged interaction tensor. That is, $\langle \mathbf{A} \rangle \neq 0$ in a uniform volume element of the sheared fluid. In such a volume element we expect that the hierarchy of motional averaging processes will yield an $\langle \mathbf{A} \rangle$ (for convenience expressed in the local 1,2,3-PAS fixed on the center of mass of a test chain) which exhibits the same anisotropy as the chain's radius of gyration tensor.

The feasibility of detecting shear-induced anisotropic NMR interactions was in fact demonstrated earlier in an uncontrolled axial annular flow experiment in which a polyisobutylene melt was doped with deuteriobenzene. In this preliminary experiment a quadrupolar splitting was observed for the benzene probe with a magnitude that decreased with time following a step strain.[8] In an effort to realize a more controlled flow field in the NMR spectrometer, a NMR-transparent rheometer was designed to generate variable stress levels in a uniform shear field, as described in the following section.

Experimental Section

NMR. Proton (90-MHz) and deuterium (13.8-MHz) NMR spectra were recorded on a commercial transverse **B**-field FT spectrometer (Bruker WH-90) with standard 10-mm variable-temperature probes running in an unlocked mode. After shimming the field in the nonspinning mode it was necessary to reshim on the free induction decay (FID) of the actual sample to remove inhomogeneities introduced by the presence of the rheometer components in the detector coil. The magnitude of the inhomogeneities and the line widths obtained after shimming are illustrated in Figure 3. The resonance is for the proton spectra of poly(dimethylsiloxane) (MW = 1.0×10^5) at ambient temperature. A limiting line width (due to residual dipolar inter-

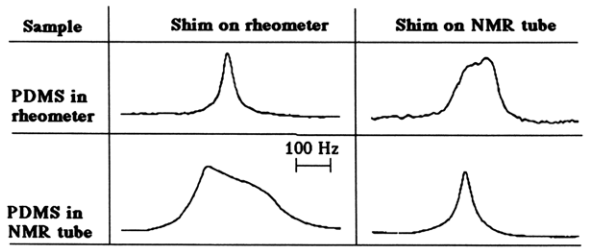

Figure 3. The proton NMR line shapes of poly(dimethylsiloxane) at 300 K in a standard 10-mm NMR tube versus that observed in the Vespel rheometer insert for different modes of shimming.

actions) with the rheometer present equivalent to that of the neat polymer in a standard 10-mm NMR tube could be achieved by careful shimming. The perturbation of the **B**-field homogeneity was noticeably larger for a rheometer constructed from the polyimide Vespel (Du Pont) than for the one constructed from Delrin, poly(methylene oxide). However, the Delrin rheometer exhibited a problematic proton background signal and all data presented here were obtained with the polyimide device. The small sample size (0.007 cm^3) precluded the convenient examination of a polymer melt doped with a small amount of a deuterated probe. Therefore in the measurements of the polymer melts described here, proton NMR line widths were examined for anisotropic residual dipolar interactions. After a rigorous sample loading procedure (see below), four FIDs (2K in size) following a $\approx$10-μs rf pulse (acquisition time $\approx$ 0.25 s with a cycle time $\approx$ 0.5 s) were averaged. Hence the minimal temporal resolution per data point (spectrum) in these steady-state experiments was about 2 s. Higher temporal resolution in combination with sinusoidal strain programs can be readily envisioned by analogy with contemporary 2-D NMR techniques, e.g., constructing 2-D maps of strain frequency versus the magnitude of the anisotropic NMR interaction.

Rheometer. A cone and plate rheometer was fabricated in the interior of a cylinder made from an engineering polymer that in turn fits into the standard 10-mm, high-resolution NMR probe (Figure 4). The rheometer itself is located within the active volume of the probe and produces minimal pertubation of the rf and magnetic fields. The schematic shown in Figure 5 facilitates a detailed description of a rheometer that can establish a uniform shear field generated by an experimentally variable shear rate. The axis of the rheometer (*A*) is perpendicular to the polymeric cylinder (NMR probe insert axis). The orientation of (*A*) may be varied continuously in a plane containing the spectrometer **B** field; i.e., the angle between the shear field and **B** may be selected. The rheometer itself consists of a 7.96-mm-diameter sample well. Referring to Figure 5, one face of the well is machined flat (B, the "plate"). The other face of the sample gap is capped by a removable cone (C) having a toothed gear machined into its periphery. (Two cone angles were used for the shearing surface: small cone angles of $\delta = 4°$ and $\delta = 8°$ ensure minimal deviation from an ideal shear flow and give the possibility of attaining the same stress level at two different angular velocities (ω) or shear rates $d\gamma/dt = \omega/\delta$.)

Drive Mechanism. The rotation of the cone relative to the plate is carried out by a positive drive: Still referring to Figure 5, a toothed Nylon drive belt (D) engages the geared periphery of the cone and a driving gear (housed in the plastic cap above that portion of the cylindrical rheometer outside of the NMR probe head). The belt is spring-loaded (the spring E is contained in the cap) in order to maintain tension in the belt which travels in grooves machined into the cylinder. A notched keyway (F) prevents twisting of the cap housing about the cylinder although the locking of the cap into the probe mounting bracket was designed so that the angle between the cone axis (A) and the magnetic field could be set deliberately. A series of commercially available aluminum miter gears (G; pictured in Figure 4b) continue the positive drive train to (H) a stainless-steel drive shaft (with brass bearings) leading out of the magnet to a variable speed, AC synchronous motor (Hurst Manufacturing, Series K) mounted on the NMR probe arm. Calibrated control of the angular velocity of the cone was established by using a control unit (Automation for Industry AD-1;

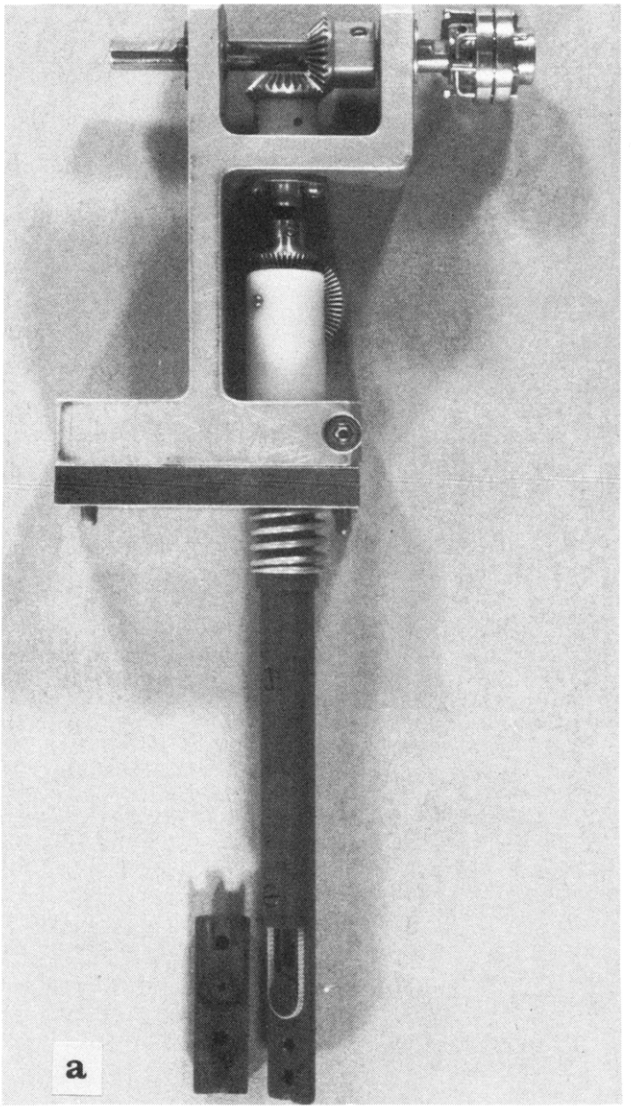

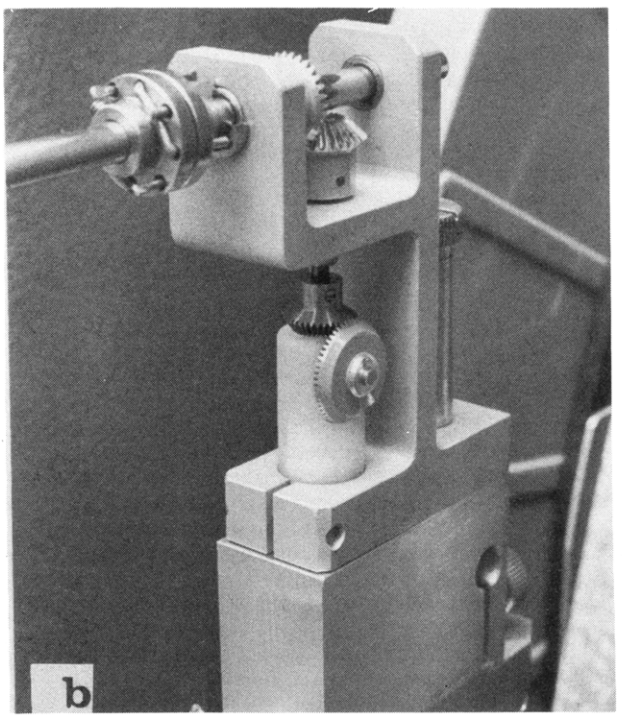

Figure 4. A photograph of the rheometer (a) and the drive mechanism (b). The latter is in place above a standard NMR probe head.

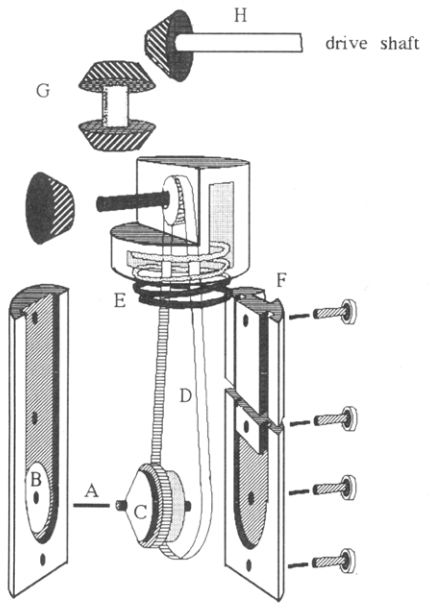

Figure 5. An exploded diagrammatic view of the rheometer illustrating the location of the cone (C) and the plate (B) in the insert. See the text for a detailed description of the components.

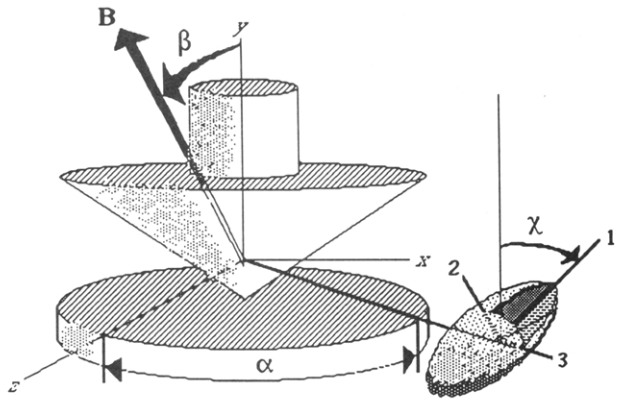

Figure 6. An illustration of the cone and plate geometry showing the relative orientation of the magnetic field **B** to the cone axis (y axis), the azimuthal orientation (the orientation of the "neutral" 3-axis relative to the z axis), and the orientation of the principal 1,2,3-axes of the averaged EFG tensor (shaded ellipsoid) at a labeled site in the deformed chain.

Electro-Sales) and two motors (angular velocities in the ranges 0.333–1.25 rpm and 8.40–37.5 rpm with maximum torque capabilities of 1.3×10^4 and 1.4×10^3 N m, respectively). This design permitted observations over a range of shear rates: 0.3–1.2 s^{-1} and 8.7–35 s^{-1} for the 4° cone and 0.15–0.6 s^{-1} and 4.3–17.5 s^{-1} for the 8° cone.

Sample Loading. A sample loading procedure was developed to eliminate the following complications: (1) the presence of voids in the sample; (2) incomplete filling of the sample well; (3) the axial play in the cone gear shaft; (4) sample leaking during shear. A loading jig was designed to ensure reproducible axial positioning between different sample loadings. An excess of sample was placed in the sample well to avoid air bubbles. After positioning the cone above the well, uniform pressure was applied by the loading jig to ensure even spreading of the sample. Complete filling is indicated by excess sample being expelled around the cone–well interface. The excess sample was carefully removed to avoid extraneous NMR signals. Following each run the cone–well interface was examined for sample leakage and those experiments exhibiting evidence of leakage were discarded. Additionally, we confirmed that the phenomena observed were independent of the shear direction and the angular starting position (phase angle) of the cone relative to the plate.

Results and Discussion

In the cone and plate rheometer employed here, a uniform shear field is generated throughout the polymer melt. Flow visualization experiments conducted with a transparent rheometer of similar dimensions confirmed that particulates imbedded in the melt exhibited regular, concentric flow paths at the shear rates used in our experiments, which would indicate an absence of turbulent flow. However, apart from the simplicity of the shear field, there are complicating aspects of this geometry that render this NMR interrogation of shear-induced anisotropy rather complex. In the flowing polymer melt (as in the deformed elastomer network), rapid segment (or probe) motion incompletely averages the tensorial NMR interactions so that $\langle \mathbf{A} \rangle$ assumes the symmetry of the local deformation gradient tensor (the radius of gyration tensor of the deformed chain).[9] For simple shear, we find for the geometry shown in Figure 6 an interaction tensor in the local PAS with the following symmetry:

$$\langle \mathbf{A} \rangle \approx \langle \mathbf{A} \rangle_a \begin{bmatrix} 1 & 0 & 0 \\ 0 & -1 & 0 \\ 0 & 0 & 0 \end{bmatrix} \tag{3}$$

In this local reference frame, the 3-axis (the radial direction in the cone and plate geometry) is the neutral direction. Moreover, the 2-axis of the PAS (along the extensional component of the shear-induced deformation) is tilted with respect to the cone axis by χ. After transforming $\langle \mathbf{A} \rangle$ to the laboratory x, y, z frame defined by the rheometer and getting the projection on **B**, we obtain the following proportionality between the quadrupolar (dipolar) splitting and the averaged EFG tensor:

$$\Delta\nu \approx \langle \mathbf{A} \rangle_a \{(3/2) \sin 2\beta \sin 2\chi \cos \alpha + [P_2(\cos \beta) + \cos^2 \alpha (P_2(\cos \beta) - 1) + (1/2)] \cos 2\chi\} \tag{4}$$

In the limit of zero shear, the angle $\chi \approx 45°$ which has serious implications: For example, $\Delta\nu = 0$ when **B** is parallel to the cone axis ($\beta = 0°$), the only condition giving a singular orientation of the uniform shear field with respect to **B**. The interaction is maximized when $\beta = 45°$. Furthermore χ will increase with increasing shear stress suggesting that, as in the case of optical measurements, NMR could be used to determine χ. Note, however, when $\beta > 0°$, $\Delta\nu$ is dependent on the azimuthal angle α. Hence, for a macroscopic cone and plate within the NMR detector coil, a superposition of $\Delta\nu(\alpha)$ will be observed. It may be further appreciated that for sufficiently rapid rotation of the cone an average over α may be effected. In short, the window of observation for rheo-NMR with the cone and plate geometry in a transverse magnetic field is rather restricted.

It is clear that the cone and plate geometry is a very complex one for the NMR experiment and interpreting resulting spectra in the case of simple shear will be less straightforward than the case for a uniaxial stress field (elongational flow). Despite these complications we attempted to determine if it is at all possible to see a change in the NMR "line shape" of a sheared polymer melt. As previously mentioned, poor signal-to-noise with the small sample volume of the rheometer precluded deuterium NMR studies of dilute probes. Therefore we used proton NMR to examine melts of poly(isobutylene) (PIB; MW = $1.8M_e$, where $M_e = 3 \times 10^4$) and poly(dimethylsiloxane) (PDMS; MW = 10^5). The large number of prox-

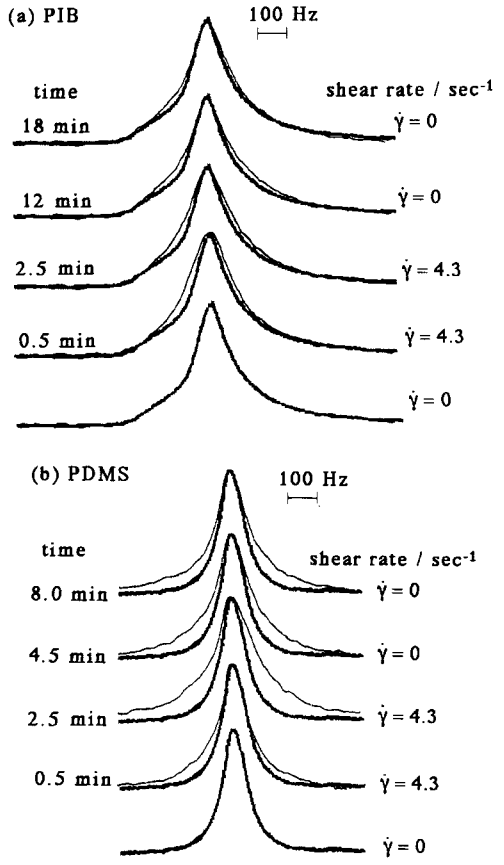

Figure 7. Proton NMR line shapes for (a) poly(isobutylene) at 345 K and (b) poly(dimethylsiloxane) at 300 K. In both series of spectra, the bottom trace (shaded line) is a superposition of five spectra in the quiescent melt; it is reproduced to serve as a reference in the spectra recorded at various times after initiating (and subsequently terminating) the shear.

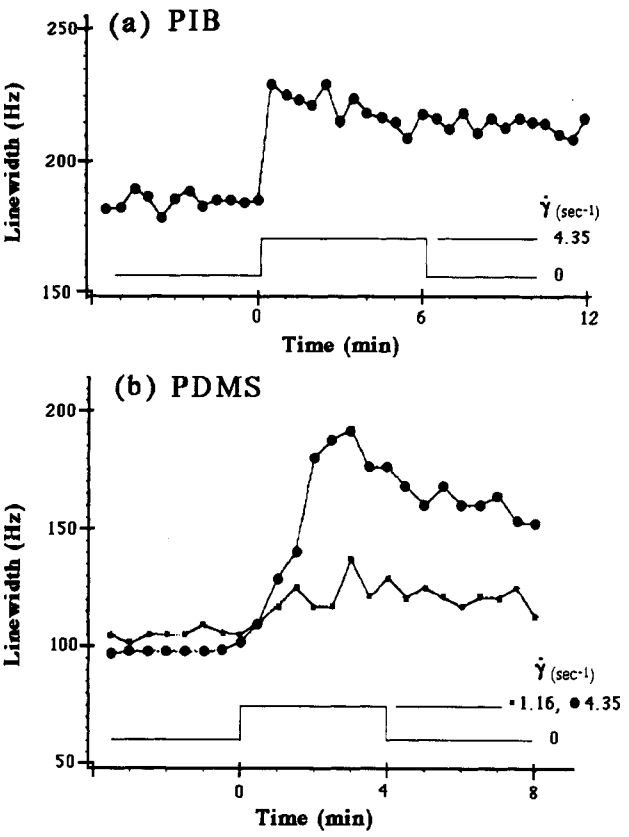

Figure 8. The temporal evolution of the apparent proton NMR line width (width in hertz at half-height) for (a) poly(isobutylene) at 345 K and (b) poly(dimethylsiloxane at 300 K. Shear commences at $t = 0$ (the initial values [$t < 0$] are representative of the reproducibility of the line width in the quiescent state; see Figure 7). The shear is subsequently stopped at a later time, and the strain profile is indicated in the diagram above the abcissa.

imate protons within the PIB and PDMS monomers implies a complex dipolar splitting pattern for $\langle D \rangle \neq 0$ and an ill-defined line shape (unlike the simple doublet characteristic of an isolated pair of dipolar coupled protons). Although at these MWs we can assume an entangled (transient) network of chains in the neat melt, dipolar interactions are effectively averaged in both polymer melts for temperatures sufficiently above T_g. The apparent line width of the proton NMR spectrum of PIB (in hertz at half-height of the signal) narrows with increasing temperature until an asymptotic, limiting line width (~175 Hz) is reached at 345 K; PDMS exhibits a limiting line width of ~100 Hz at 300 K. The resonance from these melts in the rheometer is reproducible from sample to sample showing only small changes in the linewidths in the relaxed state. The effect of the shear stress is illustrated in Figures 7 and 8 where the apparent line width is shown versus time after starting to shear the melt. This start is essentially instantaneous (~1 s) on the time scale of observed changes in the spectra. Some raw data are shown in Figure 7 with a reference, limiting line-width resonance (shaded trace) composed of the superposition of five spectra in the initially quiescent melts of the respective polymers. The reproducibility of the data prior to starting the rheometer ($t < 0$) indicates the reliability of the line-width measurements. A clear increase in the line width is observed for both PIB and PDMS after the shear is applied. This is probably a result of a change in the line shape due to a redistribution of intensity corresponding to a disturbance of an initially isotropic distribution of the residual dipolar couplings $\langle \mathbf{A} \rangle_a$. (It is conceivable that one might be able to differentiate between a shear-induced redistribution of $\langle \mathbf{A} \rangle_a$ and a shear-induced increase in the dipolar couplings by a careful examination of the FID with, for example, a Carr–Purcell pulse sequence.) More importantly, however, for both polymers the evolution of the line shapes occurs on a time scale that is large (>1 min) relative to viscoelastic time scales (<1 s) characteristic of these melts. Independent steady shear and dynamic viscosity studies indicate that we are in the regime where the longest relaxation time τ satisfies the relation $\dot{\gamma}\tau \ll 1$.[3] The disparity between the viscoelastic time scale and the reaction time observed with NMR is even more pronounced in the decay of the shear-induced broadening after stopping the shear.

Rheo-NMR may also be used to observe a shear-induced phase transformation in a polymer fluid. Poly(vinyl methyl ether) (PVME) exhibits a clear transparent phase when mixed with a few percent water at ambient temperature; raising the temperature 15 deg (315 K) causes a transformation of the PVME/H_2O mixture to an opaque melt (Figure 9a). Moreover, there is a characteristic change in the proton NMR spectrum associated with this transformation (Figure 9b). A similar change in the PVME/H_2O NMR spectrum may be observed in the rheometer when the sample is sheared at ambient temperature (Figure 9c). Estimates of the viscous heating suggests that the change in temperature during shearing should be less than 1 deg.[10] Scattering studies of shear-induced turbidity in polymer solutions indicate that comparable shifts in the transformation temperature can be attained in stressed polymer fluids.[11]

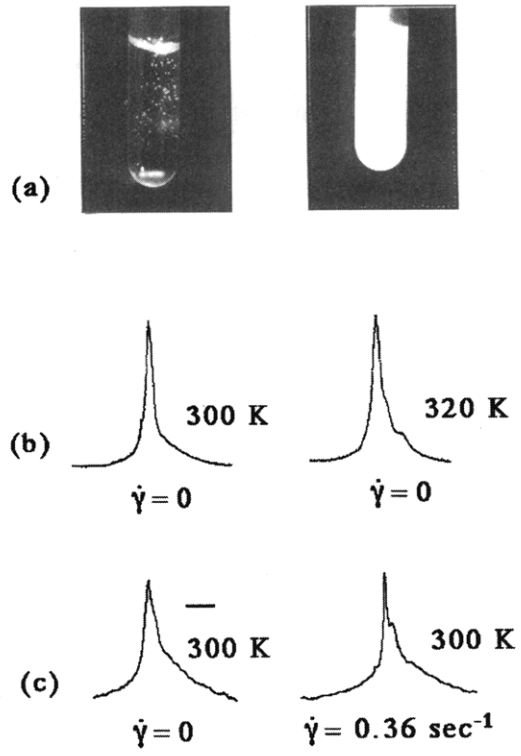

Figure 9. (a) Poly(vinyl methyl ether)–water (~5%) exhibits a clear transparent phase at ambient temperature; this phase becomes opaque on heating. (b) Temperature dependence of the proton NMR spectra of the PVME–H_2O system at zero shear. (c) Shear rate dependence of the proton NMR spectrum of the PVME–H_2O system; the spectral changes are reversible when the shearing is stopped. The scale bar is 500 Hz.

Concluding Remarks

Our evidence indicates that rheo-NMR is a potentially powerful method for studying shear-induced phenomena in bulk polymers, although a large number of difficulties had to be addressed in route to a feasible rheometer. For example, the dimensional tolerances of the cone shaft must be exact to minimize oscillatory shear stresses caused by a build-up of the normal forces generated in the rheometer and a rigorous procedure for ensuring uniform sample loading is required. The results reported here for PIB and PDMS were readily reproducible after developing a protocol for sample loading and optimizing the rheometer's dimensional stability. Similar findings were achieved with different cone angles (4° versus 8° cone angles). We find the unusually long time scales associated with the shear-induced NMR changes troublesome, but there are numerous possible explanations, e.g., surface phenomena, microscopic residual order in the absence of stress, etc. Such phenomena require more detailed study before these NMR observations can be reconciled with the known rheological time scales.

Although the cone and plate geometry is ideal for rheological studies, miniaturization of the rheometer and observing averaged second rank tensorial interactions (projected on a single axis **B**, the magnetic field direction) present some unique experimental challenges. The findings reported here together with earlier NMR studies of stressed PIB melts[8] certainly indicate that rheo-NMR is a technique worthy of further investigations. If the specificity of NMR were exploited, we foresee the possibilities of asking very detailed questions about bulk polymeric fluids in shear fields. For example, isotopic labeling could differentiate the behavior of chain ends from internal segments. Stress distributions in polydisperse mixtures (with one component labeled) could also be ascertained. Lastly, these findings suggest that the spatial variation of the magnitude of anisotropic interactions in stressed fluid phases, in combination with the rapidly developing field of NMR imaging, could be used to map out stress levels associated with a variety of strain fields imposed on macromolecular solutions, melts, and viscoelastic solids.

Acknowledgment. Robin Ball's critical insights into the complications of the cone and plate geometry were especially valuable and Monty Shaw provided sound and frequent directions during the course of our work. Our efforts were considerably facilitated by the talents of machinists T. Swol and J. Soracchi. We are indebted to Alan English for consultations about the rheometer materials and E. I. du Pont de Nemours & Co. for financial support of this research.

References and Notes

(1) Emsley, J. W., Ed. *Nuclear Magnetic Resonance of Liquid Crystals*; NATO ASI Series C; Reidel: The Netherlands, 1985; Vol. 141. Wade, C. G. *Annu. Rev. Phys. Chem.* **1977**, *28*, 47. Emsley, J. W.; Lindon, J. C. *NMR Spectroscopy Using Liquid Crystal Solvents*; Pergamon Press: Oxford, 1975.
(2) Abragam, A. *The Principles of Nuclear Magnetism*; Oxford University Press: London, 1961.
(3) Nakatani, A. I. Ph.D. *Dissertation*, University of Connecticut, 1987. Nakatani, A. I.; Samulski, E. T. In Preparation.
(4) Deloche, B.; Samulski, E. T. *Macromolecules* **1981**, *14*, 575.
(5) Dubault, A.; Deloche, B.; Herz, J. *Polymer* **1984**, *25*, 1405. Gronski, W.; Stadler, R.; Maldaner-Jacobi, M. *Macromolecules* **1984**, *17*, 741. Toriumi, H.; Deloche, B.; Herz, J.; Samulski, E. T. *Macromolecules* **1985**, *18*, 304.
(6) Sotta, P.; Deloche, B.; Herz, J. *Polymer* **1987**, *29*, 1171.
(7) Dubault, A.; Deloche, B.; Herz, J. *Prog. Colloid Polym. Sci.* **1987**, *75*, 45.
(8) Samulski, E. T. *Polymer* **1985**, *26*, 177.
(9) As described in ref 8, the projection of the incompletely averaged second rank NMR interaction tensor along the spectrometer magnet field **B** may be expressed in terms of $^2/_3$trace(**A**·**S**) where the interaction tensor **A** and the order tensor **S** are specified in a common molecular fixed frame. **S** specifies the average orientation of this frame with respect to **B** in terms of direction cosines l_i ($S_{ij} = \langle(3l_il_j - \delta_{ij})/2\rangle$). For a shear deformation in an entangled polymer fluid, A_{ij} may be identified with the partially averaged tensor within a primitive path segment $\langle \mathbf{A} \rangle_s$ if, correspondingly, S is identified with the (time-dependent) order parameter at a point s on the primitive chain, i.e., $S_{ij}\{s,t\}$. In turn, $S_{ij}\{s,t\}$ may be formally related to the shear stress in the framework of the reptation model of an entangled polymer melt (see, for example: Doi, M.; Pearson, D.; Kornfield, J.; Fuller, G. *Macromolecules* **1989**, *22*, 1488).
(10) Bird, R. B.; Armstrong, R. C.; Hassager, O. *Dynamics of Polymeric Liquids*, 1st ed.; Wiley: New York, 1977; Vol. 1.
(11) Ver Strate, G.; Phillippoff, W. *J. Polym. Sci., Polym. Lett. Ed.* **1974**, *12*, 267. See also Nakatani, A. I.; Kim, H.; Takahashi, Y.; Han, C. C. *Polym. Commun.* **1989**, *30*, 143.

Registry No. Poly(isobutylene), 9003-27-4; poly(vinyl methyl ether), 9003-09-2.